JOURNAL OF ENDOUROLOGY
Volume 36, Number 7, July 2022

Pp. 996–1003
DOI: 10.1089/end.2021.0714

Improving Burst Wave Lithotripsy Effectiveness for Small Stones and Fragments by Increasing Frequency: Theoretical Modeling and *Ex Vivo* Study

Michael R. Bailey, PhD,[1,2] Adam D. Maxwell, PhD,[1,2] Shunxiang Cao, PhD,[3] Shivani Ramesh,[1] Ziyue Liu, PhD,[4] James C. Williams, Jr., PhD,[5] Jeff Thiel, BS, RDMS,[1] Barbrina Dunmire, MS,[1] Tim Colonius, PhD,[3] Ekaterina Kuznetsova, MS,[1] Wayne Kreider, PhD,[1] Mathew D. Sorensen, MD, MS, FACS,[2,6] James E. Lingeman, MD, FACS,[7] and Oleg A. Sapozhnikov, DSc[1,8]

Abstract

Introduction and Objective: In clinical trial NCT03873259, a 2.6-mm lower pole stone was treated transcutaneously and *ex vivo* with 390-kHz burst wave lithotripsy (BWL) for 40 minutes and failed to break. The stone was subsequently fragmented with 650-kHz BWL after a 4-minute exposure. This study investigated how to fragment small stones and why varying the BWL frequency may more effectively fragment stones to dust.

Methods: A linear elastic theoretical model was used to calculate the stress created inside stones from shock wave lithotripsy (SWL) and different BWL frequencies mimicking the stone's size, shape, lamellar structure, and composition. To test model predictions about the impact of BWL frequency, matched pairs of stones (1–5 mm) were treated at (1) 390 kHz, (2) 830 kHz, and (3) 390 kHz followed by 830 kHz. The mass of fragments >1 and 2 mm was measured over 10 minutes of exposure.

Results: The linear elastic model predicts that the maximum principal stress inside a stone increases to more than 5.5 times the pressure applied by the ultrasound wave as frequency is increased, regardless of the composition tested. The threshold frequency for stress amplification is proportionate to the wave speed divided by the stone diameter. Thus, smaller stones may be likely to fragment at a higher frequency, but not at a lower frequency below a limit. Unlike with SWL, this amplification in BWL occurs consistently with spherical and irregularly shaped stones. In water tank experiments, stones smaller than the threshold size broke fastest at high frequency ($p = 0.0003$), whereas larger stones broke equally well to submillimeter dust at high, low, or mixed frequencies.

Conclusions: For small stones and fragments, increasing frequency of BWL may produce amplified stress in the stone causing the stone to break. Using the strategies outlined here, stones of all sizes may be turned to dust efficiently with BWL.

Keywords: lithotripsy, urolithiasis, urinary stones

[1]Center for Industrial and Medical Ultrasound, University of Washington, Seattle, Washington, USA.
[2]Department of Urology, University of Washington School of Medicine, Seattle, Washington, USA.
[3]Department of Mechanical Engineering, California Institute of Technology, Pasadena, California, USA.
[4]Department of Biostatistics and Health Data Science, Indiana University School of Medicine, Indianapolis, Indiana, USA.
[5]Department of Anatomy, Cell Biology, and Physiology, Indiana University School of Medicine, Indianapolis, Indiana, USA.
[6]Division of Urology, VA Puget Sound Health Care System, Seattle, Washington, USA.
[7]Department of Urology, Indiana University School of Medicine, Indiana, USA.
[8]Department of Acoustics, Physics Faculty, Moscow State University, Moscow, Russia.

Introduction

We are developing an ultrasound-based burst wave lithotripsy (BWL) system for fragmenting stones in awake subjects.[1] Unlike shock wave lithotripsy (SWL), which uses a single broadband pulse of ultrasound to fragment stones, BWL uses narrowband pulses consisting of multiple cycles of ultrasound. The amplitude of the BWL pulse is lower than with SWL and has the potential to be used as an office-based procedure.

In a clinical trial, BWL has been used to fragment stones in unanesthetized awake subjects.[2] In another trial, conducted during a subject's standard-of-care ureteroscopy procedure BWL fragmentation was visualized and quantified.[3,4] These results include a 2.6-mm stone, the smallest one targeted so far, that did not fragment. The stone was basket extracted intact and exposed for an additional 30 minutes to the same BWL settings in a water bath, with still no evidence of fragmentation. The stone was then exposed to a 650-kHz BWL pulse of the same number of cycles, pulse repetition frequency, and peak pressure. After 4 minutes, the stone broke into four fragments all ≤2 mm in largest dimension and ≤1-mm fragments within 30 minutes. With this study, we sought to explain how the change in BWL frequency contributed to fragmentation success.

Studies have shown a decrease in SWL and BWL effectiveness to break a stone if the stone is larger than the beamwidth of the pulse.[5–7] However, little has been discussed regarding a minimum stone size that can be broken. Theoretically, the smallest size fragments that can be generated using SWL are proportionate to the lithotripter pulse length. Achieving fragments smaller than the pulse length is thought to be a result of cavitation.[8] Similarly, the largest fragments produced by BWL are proportionate to the BWL wavelength, which is the inverse of frequency.[6] In other words, the higher the frequency, the smaller the fragment size, but potentially at the cost of a longer procedure to grow a denser web of cracks.

The question addressed in this article is how the choice of frequency impacts not just the fragment size, but also the size of stone that can be fragmented. The results include a calculation of the stress produced within a stone by the BWL pulse and an *ex vivo* study of breaking stones of varying sizes using two different frequencies. The outcomes help explain why this particular (2.6 mm) stone did not break clinically and provide insight into optimizing BWL to break stones to submillimeter dust that will have a high likelihood of spontaneous asymptomatic passage.

Methods

Theoretical modeling

The mechanical stresses generated by a BWL burst in a stone of size, structure, and composition similar to the clinically intact (2.6 mm) stone were estimated using a well-established linear elastic model used for investigating the fracture mechanism of SWL.[9–12] The primary plots show the stress over an initially 50 × 50 mm cross section along the centerline of the stone. For this study, the outputs include the maximum principal stress achieved within the stone, which corresponds to the maximum of all the stresses, the total strain energy in stone, and the damage potential evaluated by the Tuler-Butcher criterion[13] with a value of tensile strength of natural stone listed in Ref.[13] All are common metrics for predicting stone fracture.

Table 1. Properties Used in the Simulation to Model Renal Calculus Composition

Material	ρ, *kg/m*^{3}	c_l, *m/s*	c_t, *m/s*
Water	1000	1500	0
COM	1823	4476	2247
COD	1875	2687	1344

COD = calcium oxalate dehydrate; COM = calcium oxalate monohydrate.

Table 1 lists the properties used in the model, including density ρ, longitudinal wave velocity c_l, and shear wave velocity c.[14–16]

The applied pressure field consisted of a plane wave characterized as a single cycle (mimicking SWL) or a tone-burst (BWL) waveform of 390-kHz or 650-kHz central frequency, 10-cycle pulse duration, and 6 MPa peak negative pressure. These models attempt to simulate aspects of the above-mentioned experiments with the 2.6-mm stone and show similar behavior for frequencies above a threshold value related to the stone size. The details of the waveform representation in the model were described previously by Sapozhnikov and colleagues.[10]

Ex vivo *experiments*

The rate of stone breakage by low (390 kHz) and high (830 kHz) frequency BWL in stones ranging in size of 1–3 mm (Set 1) and 3–5 mm (Set 2) was evaluated in water bath. The 830-kHz transducer was used because it had the same beamwidth (>5 mm) of the 390-kHz transducer to be effective on stones 5 mm and smaller and a frequency predicted to be effective on stones 1 mm and larger; the 650-kHz transducer used above had a narrower beamwidth only appropriate for the 2.6-mm stone. Each set of stones was matched by size and exposed to either the low-frequency or high-frequency burst. In addition, a third set of 3–5 mm stones was exposed to a combination of low-frequency burst followed by a high-frequency burst (Mixed Set).

Stones. All stones were predominately calcium oxalate monohydrate (COM) (>95% as measured by infrared spectroscopy), and all were hydrated for more than 1 week before the experiment. All stones were weighed wet before use. COM stones are the most common type, and other stone compositions were investigated in our companion article by Sapozhnikov and colleagues.[12]

Setup. The stone was held in a water-filled depression in a tissue mimicking phantom simulating a calyx (Fig. 1). The depression was cylindrical with a 5-mm-diameter × 10-mm-deep well with a pointed bottom that ensured the stone and fragments stayed at the focus. The transducer pointed downward at the phantom in a water bath at 50% oxygen saturation.[17] The conditions were chosen to mimic thresholds for cavitation *in vivo* as measured with the 390-kHz frequency, and exposure conditions for clinical trials with 390 kHz were chosen to avoid formation of a cavitation cloud. The inline ultrasound imaging is used to detect if a cavitation cloud

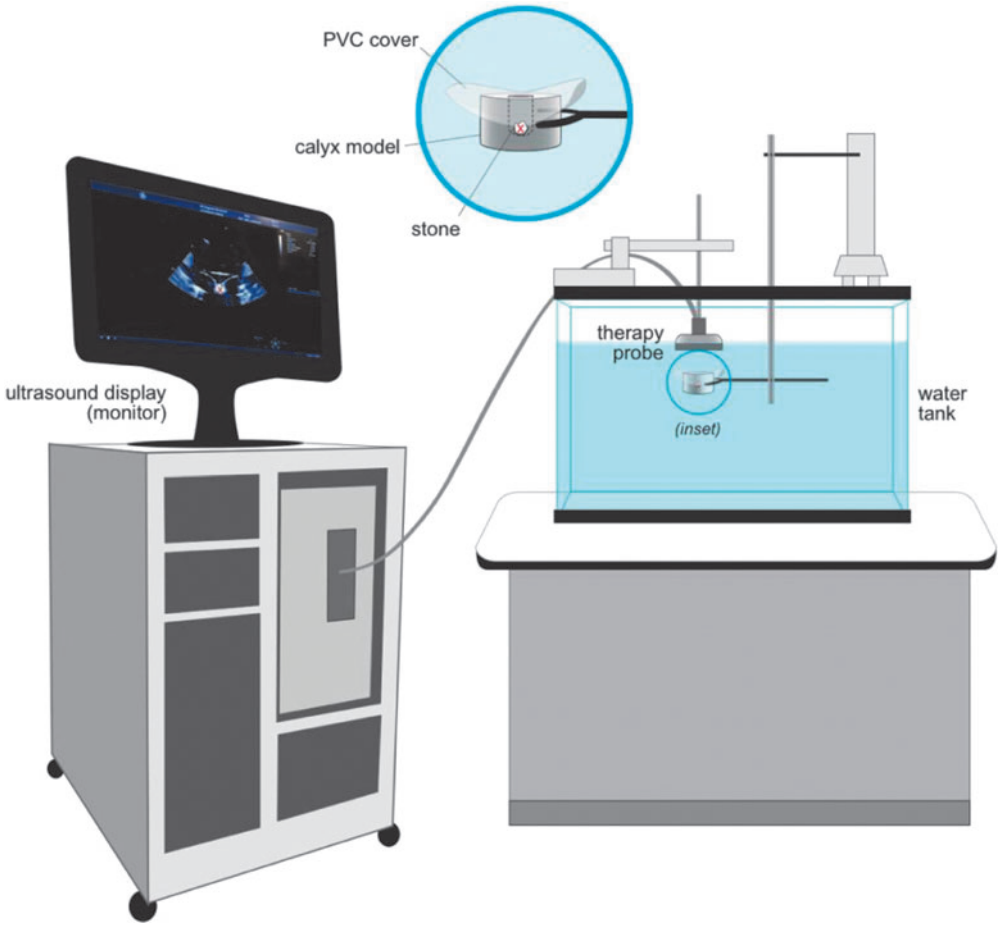

FIG. 1. Experimental setup. Color images are available online.

forms, and treatment is then paused. No cavitation clouds were observed in the current experiment with either frequency.

Fragments were removed from the phantom every 2.5 minutes and passed through a 1-mm sieve. The remaining (residual) fragments that did not pass through the sieve were weighed and then passed through a 2-mm sieve. The residual fragments that did not pass through the 2-mm sieve were again weighed. All stones >1 mm were returned to the phantom for more treatment.

Exposure parameters. The BWL therapy was delivered using two separate transducers for the different frequencies, but both had the same beamwidth, which was 6 mm and wider than the maximum dimension of all the stones. The exposure consisted of 6 MPa peak negative pressure, 20-cycle pulse duration, and 10-Hz pulse repetition frequency. This was consistent with the clinical dose taking into consideration tissue attenuation. All stones were exposed for 10 minutes maximum. In the mixed frequency case, the first 2.5-minute exposure was at low frequency and the remaining 7.5-minute exposure was at high frequency.

Analysis. The residual masses were normalized to the initial mass and averaged at each time point for each exposure, sieve size, and stone (set) size. Large stones and small stones were analyzed separately. The rates of comminution were statistically compared in two approaches: interval-censored time-to-event data and longitudinal data analysis based on the remaining percentages. Time-to-event data included two approaches—generalized log-rank and a Cox proportional hazard model for interval-censored data. The longitudinal data analysis approach was used to predict the probability outcome of complete comminution based on the remaining residual stone masses, analyzed overall and at each time point.

Linear mixed-effects models were used with a random intercept for stone level, and another random intercept at the matching level. Time was treated as a categorical variable, for the time trend is nonlinear. The frequency effects were analyzed by comparing the longitudinal mean profiles across different frequencies. All duplicate measures agreed on statistical significance (p-value <0.05), and the highest p-value is presented.

Results

The extracted stone was approximately spherical (Fig. 2a). Microcomputed tomography measured the stone as $2.6 \times 2.5 \times 1.8$ mm. The stone had a COM core surrounded by a thin calcium oxalate dihydrate (COD) shell (Fig. 2b).[18]

Theoretical modeling

Three stones were modeled: a 2.6-mm spherical COM-only stone, a 2.6-mm spherical COM stone with a COD shell,

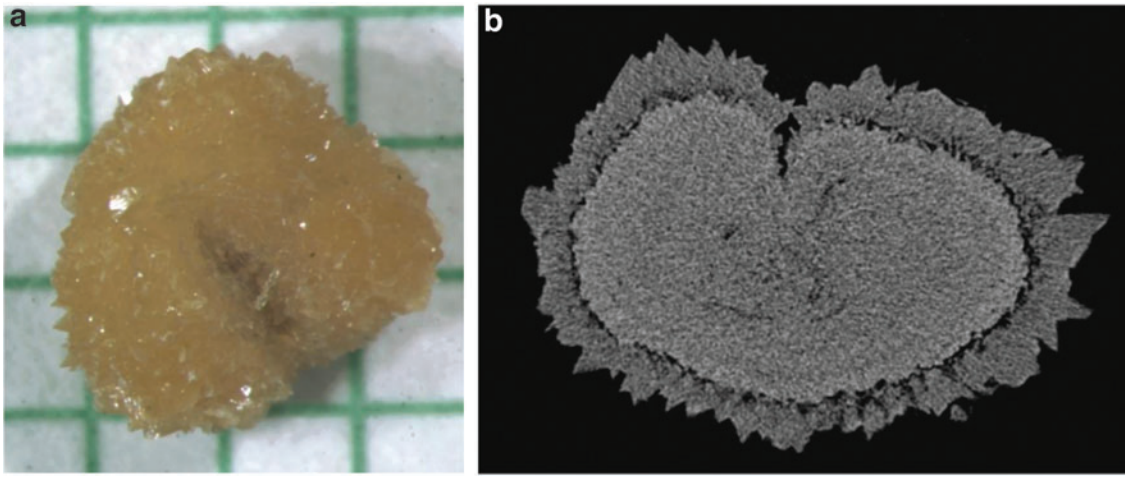

FIG. 2. **(a)** Photograph of the extracted stone on 1-mm graph paper, and **(b)** slice of a volume image of the stone made by microcomputed tomography after the *in vivo* exposure to BWL. The inner material is COM and the outer is COD. The fissure at the *top* of the stone appears to be naturally present and not caused by BWL. BWL = burst wave lithotripsy; COD = calcium oxalate dihydrate; COM = calcium oxalate monohydrate. Color images are available online.

and an asymmetric shape emulating the extracted stone. Figure 3 shows the maximum stress along the centerline of the stone. Except the last column that shows the stress, the maximum stress is normalized by the peak negative pressure of the BWL pulse to highlight the amplification of the stress within the stone. A single-cycle pulse, such as SWL, creates negligible amplification as does a 390-kHz BWL burst for this size stone. However, the 650-kHz BWL burst creates a stress within the stone that is more than five times the pressure applied. The result is consistent even when including the COD shell on the stone and the irregular nonspherical shape of the stone as shown in Figure 3.

Figure 4 shows the amplification of the stress at the center of a COM spherical stone over the applied acoustic pressure for a 10-cycle, 6 MPa BWL pulse at the same two frequencies (390 and 650 kHz) for two stone sizes. At 390 kHz, the pressure within the 2.6-mm stone more than doubled to 17 MPa. For a larger (4.5 mm) stone, the amplification was

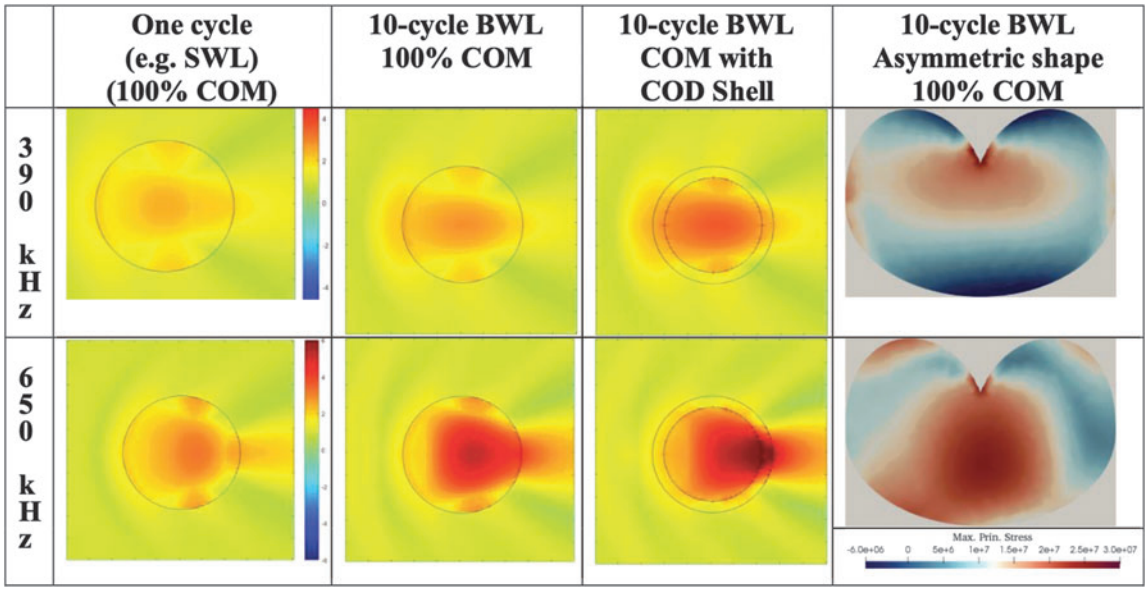

FIG. 3. Simulated image of the peak maximum principal stress along the centerline of the stone. The *upper column* shows stress induced by 390-kHz lithotripsy burst and the lower shows stress induced by a 650-kHz lithotripsy burst. The scale (−6 to 6) is maximum stress divided by the incident pressure and represents the amplification of the applied pressure. A single cycle, similar to the shape of an SWL pulse, produces little stress and negligible amplification in the 2.6-mm-diameter spherical stone regardless of the frequency. The *second column* shows the results from a 10-cycle BWL pulse, where the lower frequency produces little stress in the stone, but the higher frequency yields 5.5 times the applied pressure within the stone. Adding a COD shell (*column 3*) increases the stress within the stone slightly, because of COD's slower sound speed; however, significant amplification of the incident pressure within the stone is still only achieved at 650 kHz. The trend is similar for the irregularly shaped stone (scale in this *column* is stress, not amplification). SWL = shock wave lithotripsy. Color images are available online.

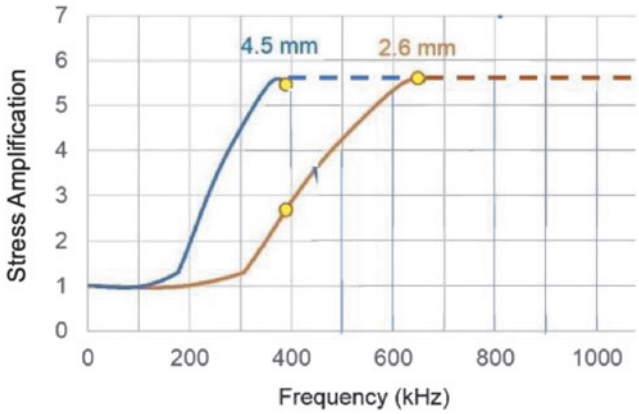

FIG. 4. Peak maximum principal stress within a COM stone normalized to the peak pressure of the applied BWL pulse *vs* BWL frequency for two stone sizes. For the 4.5-mm stone (*blue line*), the pressure amplification is more than 5.5 at both 350 and 650 kHz. However, for the smaller 2.6-mm stone (*orange line*), the amplification is 2.8 at 390 kHz, but 5.5 at 650 kHz. A *dashed line* is shown to the *right* of the peak to reflect that the amplification remains consistent, but there is a shift off-center and variations with specific resonances are not shown but are discussed further in the article by Sapozhnikov and colleagues.[12] The plots show a threshold in minimum frequency that must be used to achieve the maximum pressure amplification for a certain stone diameter. Color images are available online.

more than 5.5 times to 34 MPa. Alternatively, the amplification was 5.5 times to 34 MPa for both the 2.6- and 4.5-mm stones at the higher frequency. Thus, selection of the frequency increased the stress in the stone by a factor of five and a half to a level sufficient to break the stone. This is consistent with the result that the 390-kHz BWL did not break the 2.6-mm stone, but the 650-kHz BWL did.

Figure 5a shows the time history of the peak strain energy and damage potential inside the 2.6-mm asymmetric stone at the end of a 1-cycle or 10-cycle, 6-MPa (peak negative pressure) lithotripsy pulse for each frequency. Both indicators support that fragmentation is less effective at 390 kHz compared with 650 kHz. Similar to the results for the principal stress, the peak strain energy requires at least approximately four cycles before amplification is observed, which is why the amplification is not seen with the single-cycle lithotripsy (i.e., SWL) pulse.

Ex vivo *experiments*

Twenty stones were included within each test population for a total of 100 stones fragmented. Figure 6 (upper) shows the average mass fraction of small stone (1–3 mm) fragments >1 mm remaining at each time point (a), and the probability of the stone being completely broken to <1 mm fragments (b) based on the remaining fragments at each time point. The stones exposed to the higher (830 kHz) frequency broke the small stones faster and more completely. For all three statistical models, the fragmentation of 1–3 mm to <1 mm size at 830 kHz is statistically better than at 390 kHz ($p = 0.0003$). Because a fraction of the stones within this group start smaller than the 2 mm sieve, those data are not presented.

Figure 6 (lower) shows the mass fraction of large stone (3–5 mm) fragments over 2 mm (c) and over 1 mm (d) remaining at each time point for high, low, and mixed frequencies. There are no statistical differences ($p = 0.2055$). For this size range (3–5 mm) at these frequencies for equal beamwidths greater than the stone size, there was no detriment to using high frequency, which breaks smaller stones better, to also break larger stones. Although not statistically significant, there is a trend of improved comminution effectiveness with the mixed frequencies. The statistical results for the fraction of stones are consistent with the longitudinal data analysis.

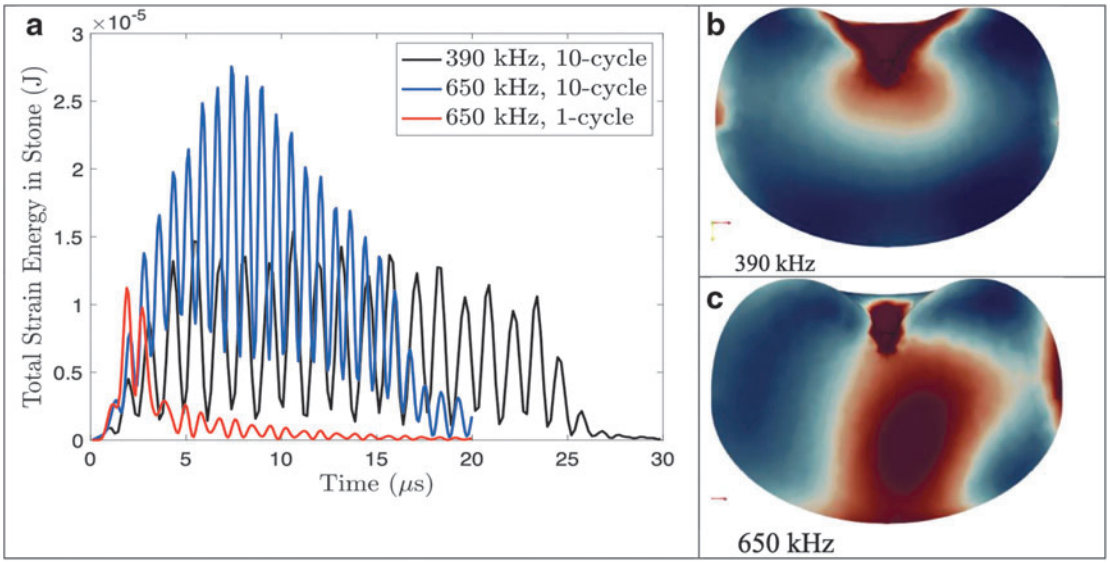

FIG. 5. Time history of the total strain energy **(a)** and damage potential with BWL at 390 kHz **(b)** and 650 kHz **(c)** inside the 2.6-mm asymmetric stone. Multiple cycles are required to reach the maximum strain energy for a given a frequency. The total strain energy is nearly double for the higher frequency in this small stone. In addition, 650-kHz BWL produces a potential damage throughout the full width of the stone, whereas 390 kHz only yields a damage potential at the stress concentrating surface feature. Color images are available online.

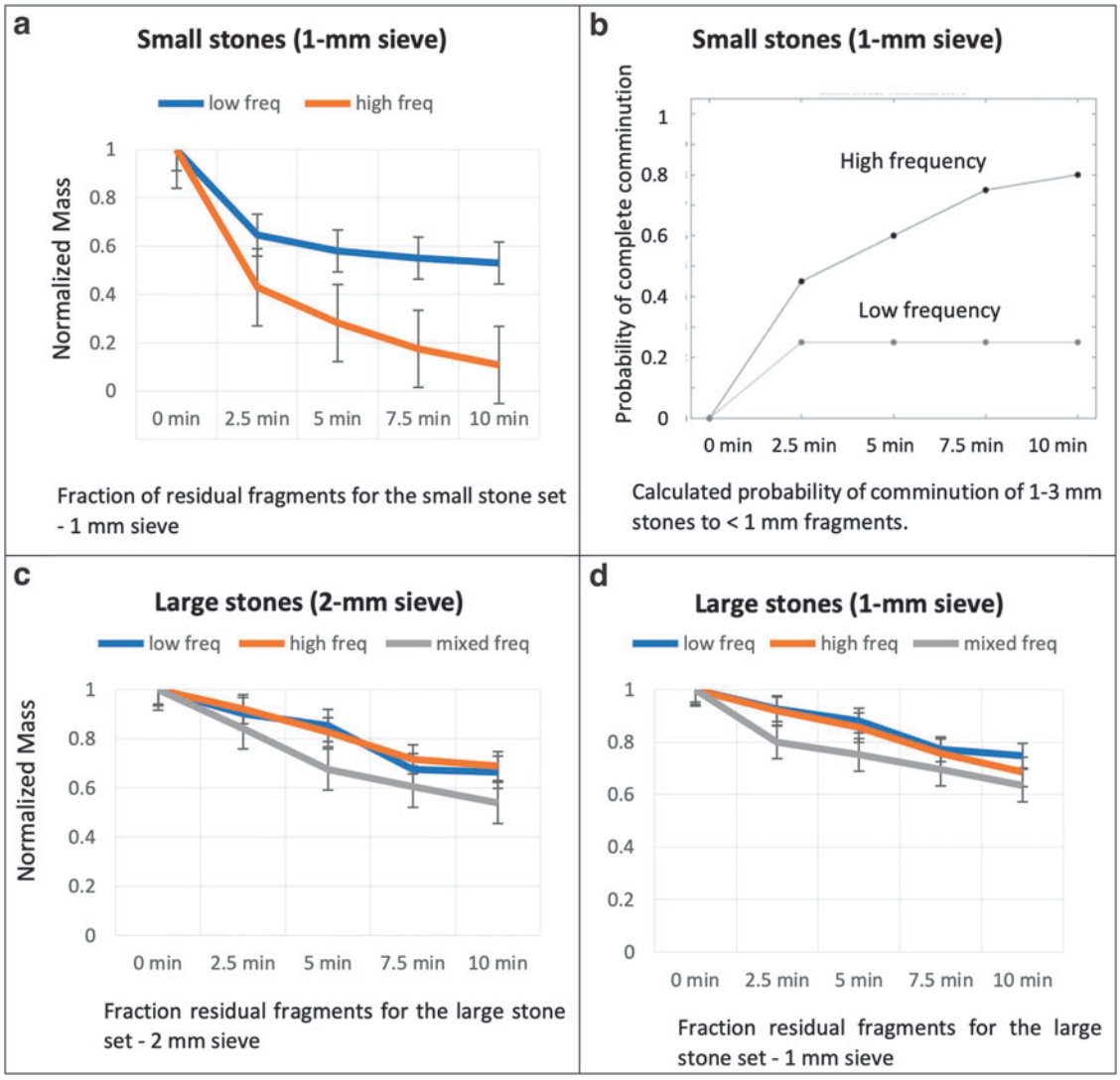

FIG. 6. The average normalized mass fraction of initially small stone (1–3 mm) fragments >1 mm remaining at each time point **(a)** and the probability of the stone being completely broken to <1 mm fragments **(b)** (*upper*). COM stones in the 1–3-mm-size range exposed to the higher frequency (830-kHz) BWL burst broke faster and more completely than similar stones exposed to the lower frequency (390-kHz) BWL burst ($p = 0.0003$). The calculated probability curve for the 390-kHz frequency flattened after 2.5 minutes, indicating the stones were not breaking further with additional exposure. The lower row shows the average normalized mass fraction of initially large stone (3–5 mm) fragments >2 mm **(c)** and 1 mm **(d)** remaining at each time point (*lower*). There are no statistical differences in rate of fragmentation between large stones exposed to low-frequency (390 kHz) BWL, high-frequency (830 kHz) BWL, or low frequency (2.5 minutes) followed by high frequency (mixed) ($p = 0.2055$). The results suggest that although it may not be possible to break a small stone at low frequency, it may be possible to use a higher frequency over a broad range of stone sizes (1–5 mm), without a loss of fragmentation effectiveness. Color images are available online.

Only one time point (at 5 minutes) was found to be significant, but significance was lost when the model was adjusted for multiplicity.

Discussion and Conclusions

Theoretical modeling and *ex vivo* experiment showed a statistically significant benefit of fragmenting small, ≤3 mm, stones using multiple cycles at a higher frequency relative to a lower frequency capable of breaking a 3–5-mm stone. This concept potentially contributed to the lack of fragmentation of a small, 2.6 mm, stone clinically at 390 kHz. The increase in fragmentation effectiveness correlates with an amplification of the incident pressure within the stone. The threshold frequency at which amplification initiates is approximately the ultrasound wave speed divided by stone size. Above the threshold frequency, the pressure of the applied BWL in the simulation was amplified five and a half times.

Amplification was consistent for the stone shape, structure, and composition. Ultimately, on average, 87% of the stone mass of 1–3-mm stones and 30% of the stone mass of 3–5-mm stones were broken to submillimeter dust in 10 minutes. For the conditions tested, we suspect particularly a beam-width larger than the stone, the high frequency was not slower

than low frequency at breaking the larger stones, and the one method of mixing frequencies that was tested might indicate that mixing frequencies may accelerate comminution to dust.

Although 4-mm residual fragments have historically been considered insignificant, modern ureteroscopy techniques often aim to dust the stone to 1-mm fragments or smaller, and as such, the clinical implications of this work are twofold. One, a potential application for BWL is the fragmentation of small symptomatic or asymptomatic stones or residual fragments before they require surgical intervention. We are embarking on a new randomized-controlled trial (NCT04796792) to test BWL and ultrasonic propulsion[19] together to facilitate clearance of small kidney stones; this work provides guidance toward selecting a frequency effective for small stones. Two, changing the BWL frequency as the stone breaks has the potential to more efficiently break-even large stones to dust. In this case, by starting with a lower frequency to rapidly generate fragments and then transitioning to a higher frequency to turn the fragments to fine dust.

Our modeling calculations were limited here to COM stones with no attenuation and uniform composition. The mechanism of action described here is the reverberation of sound within the stone allows for focusing and constructive interference of waves and reflections. The attenuation of stones is known within a range considered with our model in a physics-centered companion article.[12] Were attenuation much greater than that range, then the waves would be too quickly absorbed to reverberate and obtain the stress amplifications reported here.

Likewise, linear elastic models are used to predict the stress, with the highest stresses having the highest probability of growing cracks. The cracks or other heterogeneities other than irregular shapes and lamellar structures were not considered here. However, cracks such as surface features related to irregular shapes concentrate the stress that created them, and tone-burst reflections from cracks can also further add to regions of high stress throughout the stone.[16] The companion article shows that the amplification occurs for stones of different homogeneous compositions and a range of parameters suitable for heterogeneous stones and can be greater than the amplification seen for COM stones.[12] COM stones appear to have the highest threshold frequency; thus, selecting an operational frequency for a COM stone should also be effective for stones of the same size, but different composition.[12]

The primary limitation of the current study is that small stones were studied because the focus was on the range of stone sizes where higher than the current clinical frequencies were beneficial. Although no stones larger than 5 mm were broken here, it was shown that stones up to 5 mm could be broken to dust and hinted that the process might be accelerated by using a lower followed by a higher frequency. It appears the fragments created from a larger stone are slightly smaller than the threshold size for a small stone to be broken at the same frequency, indicating that this threshold may also be related to the size of fragments generated from a large stone.

This article neglects cavitation and focuses on elastic waves, as these have been demonstrated to correlate with the location and presence of fractures. Although cavitation, which is neglected in the model, and surface waves, which are included in the model, are thought to contribute to stone erosion and may initiate fracture, stones and fragments do not appear to erode significantly in BWL, particularly hard stones such as COM, but rather fracture into fragments as seen in this study.[7,12,16,20] In addition, cavitation would be expected to have the opposite effect to that measured: cavitation decreases with frequency yet here fragmentation increased with frequency.

The practical limitation to clinical application is the transducer. An encouraging conclusion of this study is that the frequency does not have to be tuned for a specific stone, only selected to be above a threshold value to achieve higher stress. However, it is easier to make a broad beam at lower frequency, and all transducers are limited to isolated or limited ranges of frequencies and cannot be used at all frequencies of potential interest.[21]

Nevertheless, techniques exist to make the BWL beam broader.[21] Also, nonlinear acoustics can be used to generate waves that contain several harmonic frequencies, and transducers often work at their fundamental frequency and at a frequency three times higher, providing ways of obtaining low and high frequencies without changing transducers. In addition, higher frequency is more readily attenuated by tissue, but even for a large skin-to-stone distance with ultrasound (10 cm), the energy loss is 7% at 390 kHz and 13% at 830 kHz.[22]

In conclusion, a small stone did not break after a 40-minute BWL exposure at one frequency, but then broke completely after a 4-minute exposure to a higher frequency with the same pulse duration, pulse repetition frequency, and incident pressure level. The result is consistent with theoretical elastic wave modeling that shows amplification of stone stress beyond the applied acoustic pressure in the stone above a threshold frequency for a given stone size. In the simulation presented here, the amplification was greater than five times the applied pressure and occurred for stones of different compositions, structures, and shapes. Overall, the work supports that adjusting BWL frequency can accelerate stone comminution and enhance fragmentation to submillimeter fragments.

Authors' Contributions

All authors contributed to the concept and design of the study, acquisition of data, analysis and interpretation of data, drafting the article or revising it critically for intellectual content, and final approval of the version to be published.

Author Disclosure Statement

M.R.B., A.D.M., B.D., and M.D.S. have equity in, and consulting agreements with, SonoMotion, Inc., which licensed the reported technology from the University of Washington for commercialization.

Funding Information

This work is supported by the NIH NIDDK Program Project grant P01 DK04331.

References

1. Chen TT, Samson PC, Sorensen MD, et al. Burst wave lithotripsy and acoustic manipulation of stones. Curr Opin Urol 2020;30:149–156.

2. Hall MK, Thiel J, Dunmire B, et al. Feasibility study of using point of care ultrasonic propulsion and burst wave lithotripsy (BWL) to noninvasively treat symptomatic ureteral stones. J Urol 2022 (in press).
3. Harper JD, Metzler IS, Hall MK, et al. First-in-human burst-wave lithotripsy (BWL) for kidney stone comminution. J Endourol 2021;35:506–511.
4. Harper JD, Lingeman JE, Sweet RM, et al. Fragmentation of stones by burst wave lithotripsy in the first nineteen humans. J Urol 2022;207:1067–1076.
5. Eisenmenger W. The mechanisms of stone fragmentation in ESWL. Ultrasound Med Biol 2001;27:683–693.
6. Sapozhnikov OA, Maxwell AD, MacConaghy B, et al. A mechanistic analysis of stone fracture in lithotripsy. J. Acoust Soc Am 2007;112:1190–1202.
7. Maxwell AD, Cunitz BW, Kreider W, et al. Fragmentation of renal calculi *in vitro* by burst wave lithotripsy. J Urol 2015;193:338–344.
8. Zhang Y, Nault I, Mitran S, et al. Effects of stone size on the comminution process and efficiency in shock wave lithotripsy. Ultrasound Med Biol 2016;42:2662–2675.
9. Cleveland RO, Sapozhnikov OA. Modeling elastic wave propagation in kidney stones with application to shock wave lithotripsy. J Acoust Soc Am 2005;118:2667–2676.
10. Sapozhnikov OA, Maxwell AD, Bailey MR. Modeling of photoelastic imaging of mechanical stresses in transparent solids mimicking kidney stones. J Acoust Soc Am 2020; 147:3819–3829.
11. Cao S, Zhang Y, Liao D, et al., Shock-induced damage and dynamic fracture in cylindrical bodies submerged in liquid. Int J Solids Structures 2019;169:55–71.
12. Sapozhnikov OA, Maxwell AD, Bailey MR. Maximizing mechanical stress in small urinary stones during burst wave lithotripsy. J Acoust Soc Am 2021;150:4203–4212.
13. Tuler FR, Butcher BM. A criterion for the time dependence of dynamic fracture. Int J Fract 1968;4:431–437.
14. Cohen NP, Whitfield HN. Mechanical testing of urinary calculi. World J Urol 1993;11:13–18.
15. Zhong P, Chuong CJ, Preminger GM. Propagation of shock waves in elastic solids caused by cavitation microjet impact. II: Application in extracorporeal shock wave lithotripsy. J Acoust Soc Am 1993;94:29–36.
16. Maxwell AD, MacConaghy B, Bailey MR, et al. An investigation of elastic waves causing stone fracture in burst wave lithotripsy. J Acoust Soc Am 2020;147:1607–1622.
17. Ramesh S, Chen TT, Maxwell AD, et al. *In vitro* evaluation of urinary stone comminution with a clinical burst wave lithotripsy (BWL) system. J Endourol 2020;34:1167–1173.
18. Williams JC, Jr., Lingeman JE, Daudon M, *et al*. Using micro computed tomographic imaging for analyzing kidney stones. C R Chim 2021;24, DOI: 10.5802/crchim.89.
19. Harper JD, Cunitz BW, Dunmire B, et al. First-in-human clinical trial of ultrasonic propulsion of kidney stones. J Urol 2016;195:956–964.
20. Gaoming X, Xiaojian M, Cosima L, et al. Variations of stress field and stone fracture produced at different lateral locations in a shockwave lithotripter field. J Acoust Soc Am 2021;150:1013–1029.
21. Randad A, Ghanem MA, Bailey MR, et al. Design, fabrication, and characterization of broad beam transducers for fragmenting large renal calculi with burst wave lithotripsy. J Acoust Soc Am 2020;148:44–50.
22. U.S. Department of Health and Human Services, Food and Drug Administration, Center for Devices and Radiological Health Guidance Document, Marketing Clearance of Diagnostic Ultrasound Systems and Transducers: Guidance for Industry and Food and Drug Administration Staff, Document issued on: 2019;27:36. https://www.fda.gov/regulatory-information/search-fda-guidance-documents/marketing-clearance-diagnostic-ultrasound-systems-and-transducers (accessed June 2, 2022).

Address correspondence to:
Michael R. Bailey, PhD
Applied Physics Laboratory
Center for Industrial and Medical Ultrasound
University of Washington
Seattle, WA 98105
USA

E-mail: bailey@apl.washington.edu

Abbreviations Used

BWL = burst wave lithotripsy
COM = calcium oxalate monohydrate
COD = calcium oxalate dehydrate
SWL = shock wave lithotripsy